ELECTRONIC SUPPORTING INFORMATION

The peculiarities of complex formation and energy transfer processes in lanthanide complexes with 2-(tosylamino)benzylidene-*N*-benzoylhydrazone

Anton D. Kovalenko[a], Ivan S. Bushmarinov[b], Anatolii S. Burlov[c], Leonid S. Lepnev[d], Elena G. Ilina[e], and Valentina V. Utochnikova[a,d]

[a] M. V. Lomonosov Moscow State University
Leninskiye Gory 1-3, Moscow, Russian Federation 119991

[b] A. N. Nesmeyanov Institute of Organoelement Compounds
Russian Academy of Sciences, Vavilova St. 28, Moscow, Russian Federation 119991

[c] Institute of Physical and Organic Chemistry
Southern Federal University, Stachki Ave. 194/2, Rostov-on-Don, Russian Federation 344090

[d] P. N. Lebedev Physical Institute, Russian Academy of Sciences
Leninskiy Prospekt 53, Moscow, Russian Federation 119991

[e] Altai State University
61 Lenina, Barnaul, Russian Federation 656049

Abstract: Depending on the local excess of lanthanide ion (Ln = Lu, Yb, Er, Dy, Tb, Gd, Eu, Nd) or 2-(tosylamino)-benzylidene-*N*-benzoylhydrazone (H_2L), lanthanide complexes, containing either mono-deprotonated ligand ($Ln(HL)_2X$, X = Cl, NO_3) or both mono- and dideprotonated ligands (Ln(L)(HL)) were preparatively obtained. The crystal structures of $Lu(HL)_2Cl$, $Yb(L)(HL)(H_2O)_2$, $Yb(L)(HL)(EtOH)_2(H_2O)$ and Er(L)(HL), determined by single crystal diffraction data or from powder diffraction data using Rietveld refinement, have shown the surprising resemblance. The studying of luminescence temperature dependence of $Eu(HL)_2Cl$ and Eu(L)(HL) showed that europium luminescence is quenched by thermally-activated $^5D_0 \rightarrow T_1$ energy transfer. The luminescent thermometers based on these complexes demonstrated the sensitivity up to 7.7% at 85K which is the highest value above liquid-nitrogen temperatures obtained to date.

Absorption spectroscopy

Absorption spectra of the lanthanide complexes in DMSO solution were obtained using single-beam spectrophotometer SF-2000 (OKB Spectr) (l = 10.0 mm) in the range 250-1000 nm.

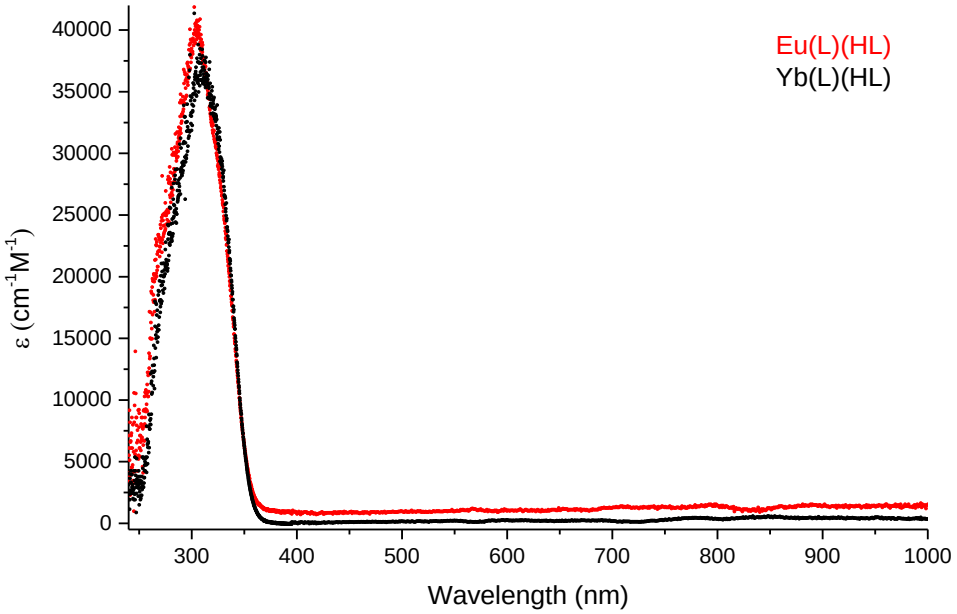

Figure 1 Absorption spectrum of Eu(L)(HL) in DMSO

Diffuse reflection spectroscopy

Diffuse refection spectra were recoded using Perkin Elmer LAMBDA 950 spectrometer in the range 200 – 1150 nm.

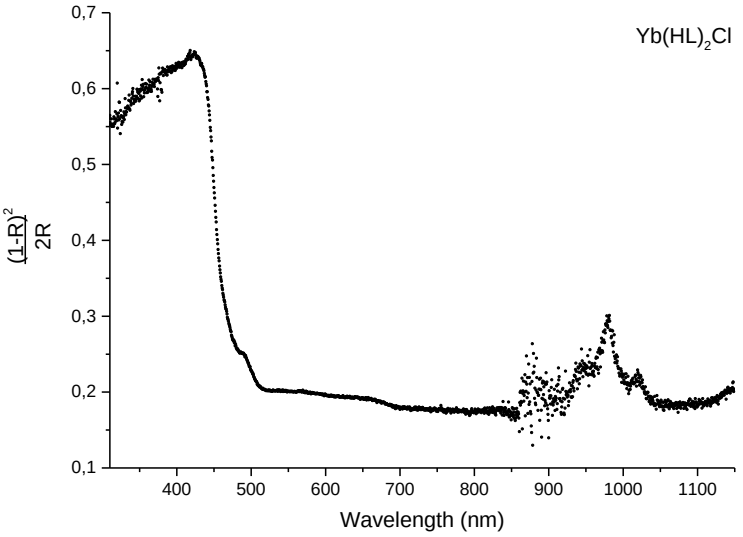

Figure 2 The DR spectrum of Yb(HL)$_2$Cl

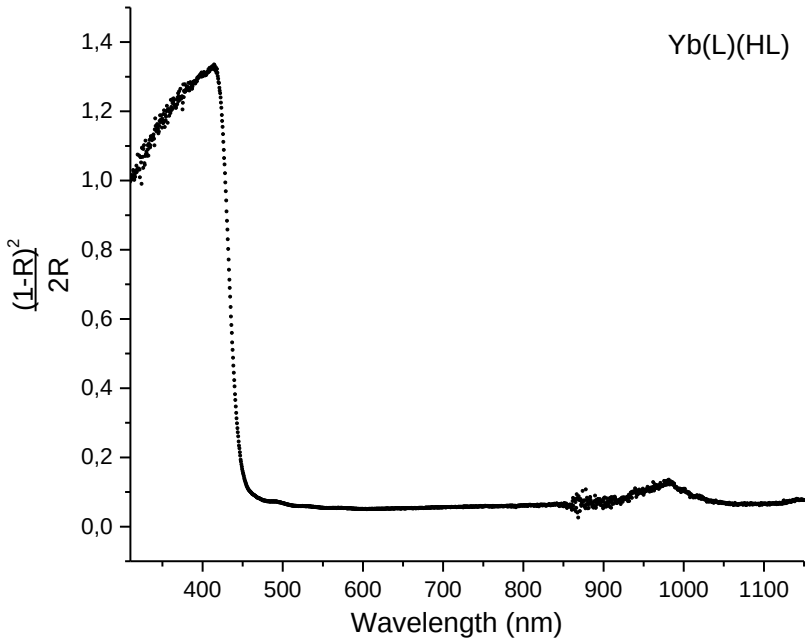

Figure 3 The DR spectrum of Yb(L)(HL)

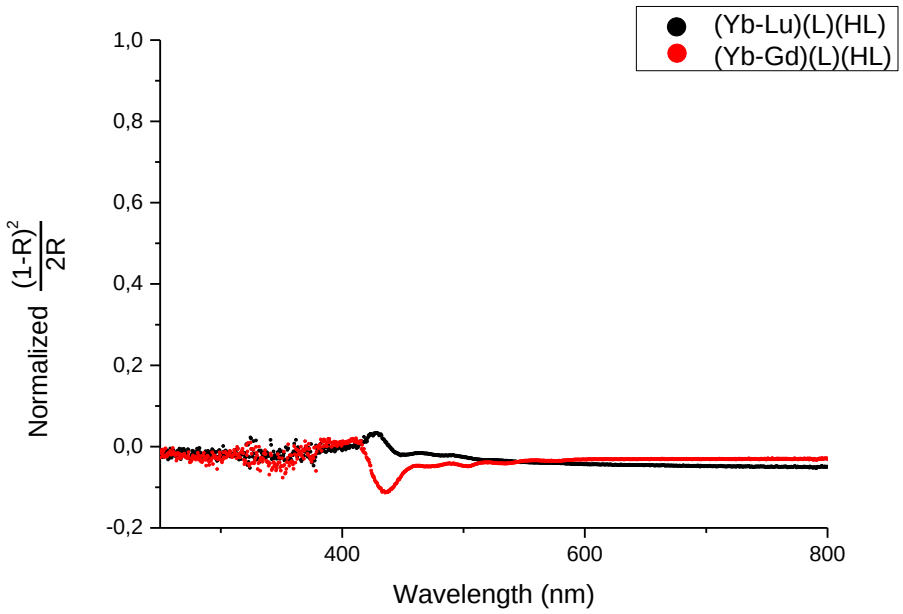

Figure 4 The difference between normalized DR spectra of Yb(L)(HL) and Lu(L)(HL), Gd(L)(HL)

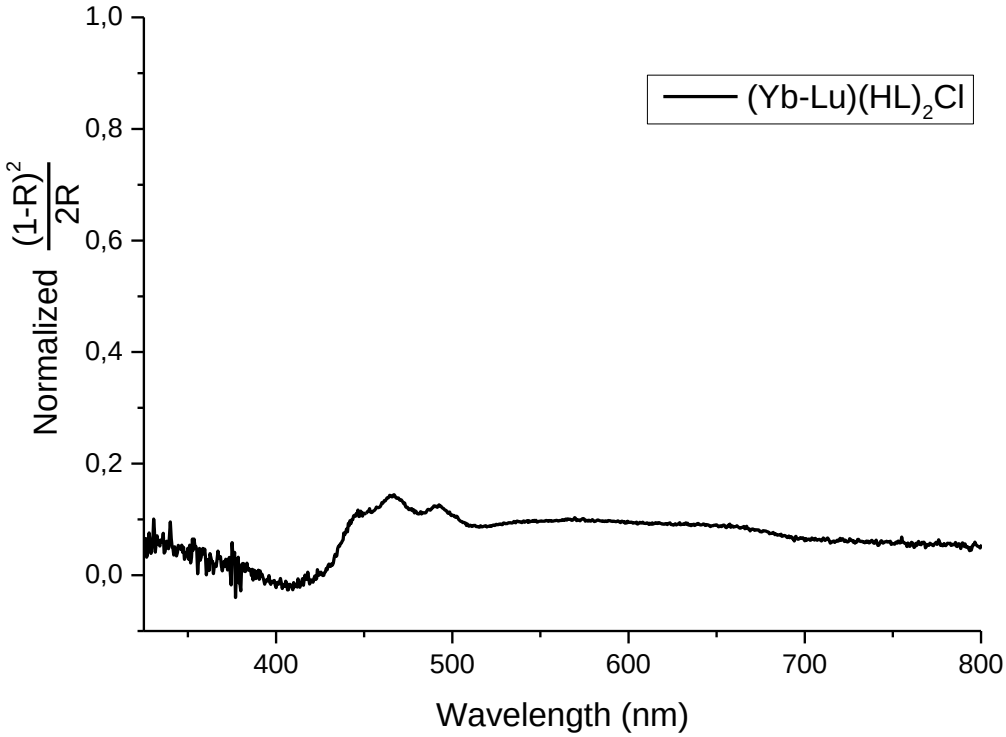

Figure 5 The difference between normalized DR spectra of Yb(HL)$_2$Cl and Lu(HL)$_2$Cl

Crystallographic data

The single crystal measurements were performed on Bruker APEX II (Mo radiation) and Bruker APEX II DUO (Cu radiation, microfocus source, used for Yb(L)(HL)$(EtOH)_2(H_2O)$) CCD diffractometers. All single crystal structures were solved using SHELXT [1] and refined using SHELXL [2,3].

Structure for Er(L)(HL) was determined form powder data. The diffraction pattern was collected using Cu $K\alpha^1$ radiation on a Bruker D8 Advance Vario powder diffractometer equipped with a Ge(111) monochromator and a LynxEye 1D silicon strip detector. The powder pattern was indexed using the SVD-Index algorithm[4] as implemented in TOPAS 5[5]. The structure was solved by Parallel Tempering as implemented in FOX[6] using two rigid bodies with torsions allowed to vary, one corresponding to a free ligand and the other consisting of a ligand linked by two nitrogen atoms to the metal atom. Further refinement was carried out in TOPAS 5, with restraints on all covalent bonds and bond angles between non-metal atoms. A weighting scheme by Toraya[7] with *e*=3.5 was used during refinement for optimal treatment of weaker reflections. The refinement was restraint-consistent[8] with half uncertainty window HUW=0.08(4) indicating a highly reliable structural model.

The final refined unit cell parameters and refinement indicators for Er(L)(HL) at K_1 = 8 (root mean square deviation from restraints on bond lengths of 0.0054 Å) are as follows **Ошибка! Источник ссылки не найден.**: $C_{42}H_{35}ErN_6O_6S_2$ (M =951.16 g/mol): monoclinic, space group $P2_1/c$ (no. 14), a = 18.8998(3) Å, b = 9.85077(15) Å, c = 25.1072(4) Å, β = 122.4174(9)°, V = 3945.95(11) Å^3, R_{wp} = 3.44%, R'_{wp} = 5.10 %, R_p = 3.49%, R'_p = 4.31 %, R_{Bragg} = 2.30%.

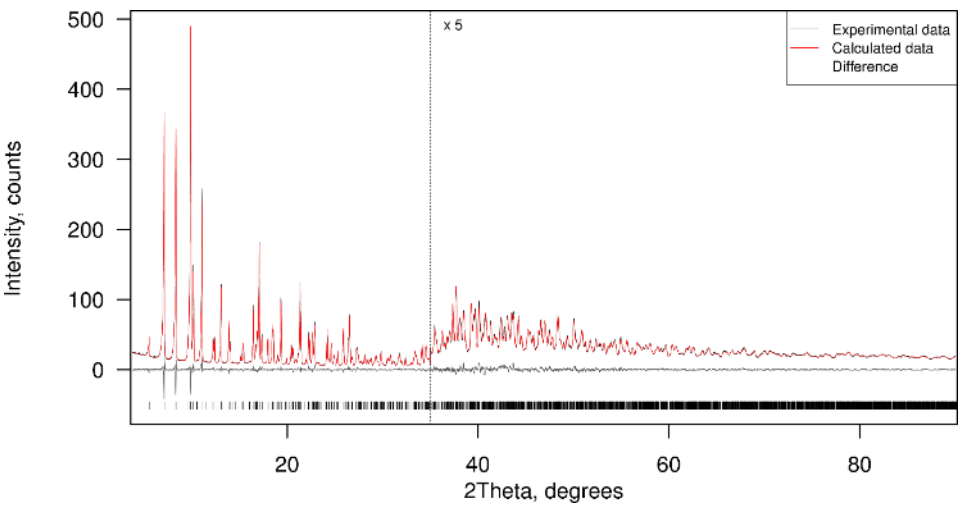

Figure 6 The Rietveld fit for Er(L)(HL).

Table 1. Crystal data and structure refinement for $Lu(HL)_2Cl$, Er(L)(HL), Yb(L)(HL)$(C_2H_5OH)_2(H_2O)$, Yb(L)(HL)$(H_2O)_2$.

Identification code	**$Lu(HL)_2Cl$**	**Er(L)(HL)**	**Yb(L)(HL)$(C_2H_5OH)_2(H_2O)$**	**Yb(L)(HL)$(H_2O)_2$**
Empirical formula	$C_{42}H_{36}ClN_6O_6S_2Yb$	$C_{42}H_{35}ErN_6O_6S_2$	$C_{46}H_{49}N_6O_9S_2Yb$	$C_{42}H_{39}N_6O_8S_2Yb$
Formula weight	993.38	951.16	1067.07	992.95
Temperature/K	120	298	120	100
Crystal system	triclinic	monoclynic	triclinic	triclinic
Space group	P-1	$P2_1/c$	P-1	P-1
a/Å	10.6091(7)	18.90072	10.7608(6)	12.530(3)
b/Å	11.4231(7)	9.851312	12.5093(7)	15.640(3)
c/Å	17.4138(11)	25.10557	17.4399(10)	22.612(5)
α/°	87.312(2)	90	77.5710(10)	103.12(3)
β/°	73.030(2)	122.4146	83.1210(10)	101.74(3)
γ/°	85.7230(10)	90	75.2430(10)	93.34(3)
Volume/$Å^3$	2012.1(2)	3946.239	2211.7(2)	4200.2(16)
Z	2	4	2	4
ρ_{calc}g/cm^3	1.640	1.601	1.602	1.570
μ/mm^{-1}	2.551	5.368	2.273	5.544
F(000)	994.0	-	1082.0	1996.0
Crystal size/mm^3	0.21 × 0.2 × 0.15	-	0.13 × 0.12 × 0.1	0.06 × 0.05 × 0.04
Radiation	MoKα (λ = 0.71073)	CuKα~1~ (λ = 1.540596)	MoKα (λ = 0.71073)	CuKα (λ = 1.54178)
2Θ range for data collection/°	3.576 to 52.742	-	3.788 to 56.562	4.116 to 135.786
Index ranges	$-13 \le h \le 13$, $-13 \le k \le 14$, $-21 \le l \le 21$	-	$-14 \le h \le 14$, $-16 \le k \le 16$, $-23 \le l \le 23$	$-14 \le h \le 12$, $-18 \le k \le 18$, $-27 \le l \le 25$
Reflections collected	20050	-	26258	42661
Independent reflections	8227 [R_{int} = 0.0546, R_{sigma} = 0.0775]	-	10988 [R_{int} = 0.0630, R_{sigma} = 0.0900]	14318 [R_{int} = 0.0621, R_{sigma} = 0.0651]
Data/restraints/parameters	8227/2/533	-	10988/3/597	14318/160/1121
Goodness-of-fit on F^2	1.045	-	0.984	1.027
Final R indexes [I>=2σ (I)]	R_1 = 0.0447, wR_2 = 0.0804	-	R_1 = 0.0431, wR_2 = 0.0806	R_1 = 0.0620, wR_2 = 0.1558
Final R indexes [all data]	R_1 = 0.0651, wR_2 = 0.0874	-	R_1 = 0.0618, wR_2 = 0.0859	R_1 = 0.0929, wR_2 = 0.1757
Largest diff. peak/hole / e $Å^{-3}$	1.77/-1.14	-	1.55/-1.25	2.36/-0.63

Thermal analysis

Thermal analysis was carried out on a thermoanalyzer STA 409 PC Luxx (NETZSCH, Germany) in the temperature range of 20-1000 °C in argon atmosphere, heating rate 10 °/min.

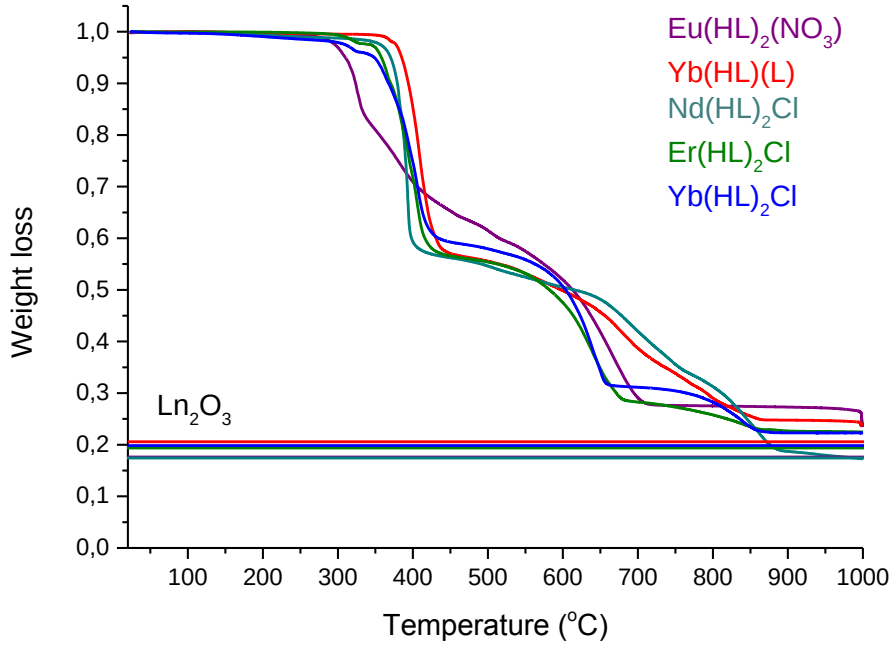

Figure 7 Thermal analysis of the complexes

XRD powder diffraction patterns

X-ray powder diffraction (XRD) measurements were performed on a Rigaku D/MAX 2500 diffractometer in the 2θ range 5–80° with Cu Kα radiation (λ = 1.54046 Å) and on a Bruker D8 Advance diffractometer (Vario geometry) equipped with a Cu Kα1 Ge(111) focusing monochromator and a LynxEye one-dimensional position-sensitive detector. The powder X-ray diffraction patterns were indexed using TOPAS 5.0 software.

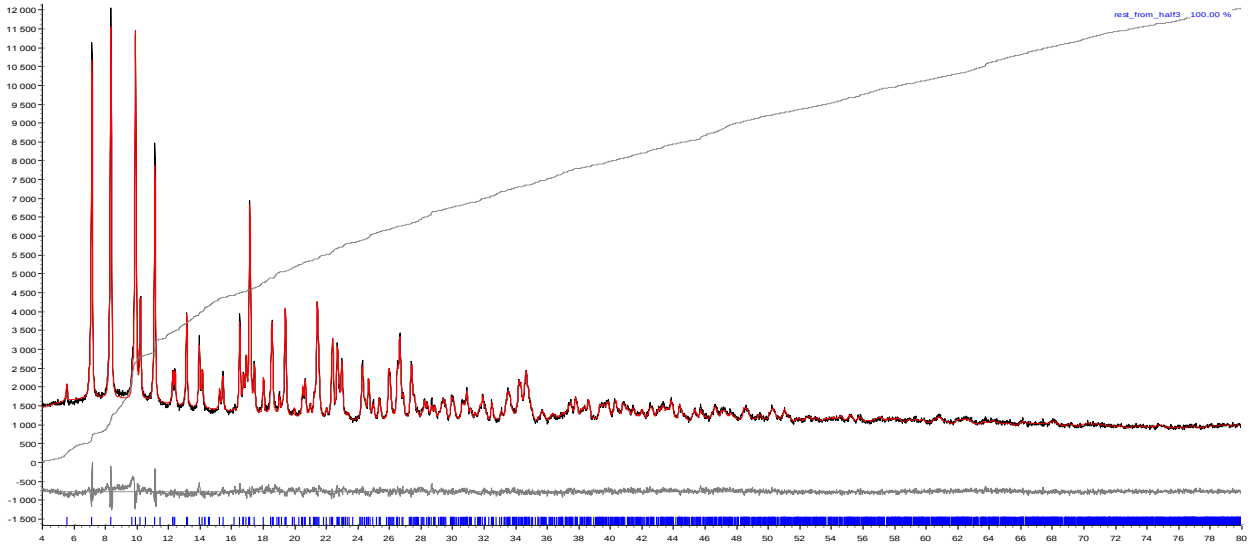

Figure 8 XRD patterns of Lu(L)(HL)

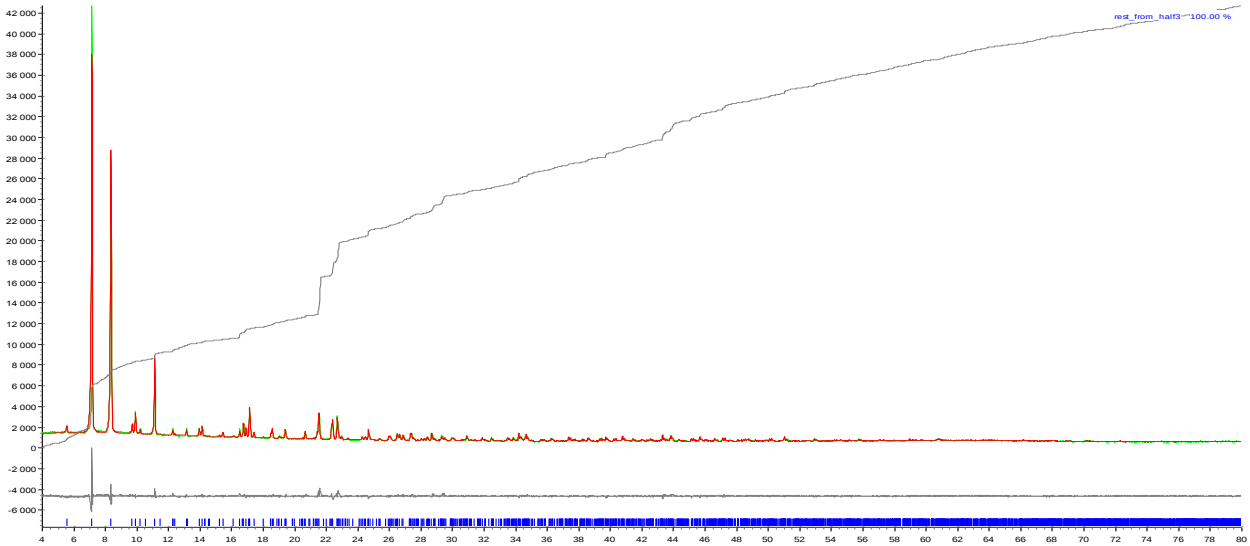

Figure 9 XRD patterns of Yb(L)(HL). The sample was not grinned that leaded to the preferential crystals orientations.

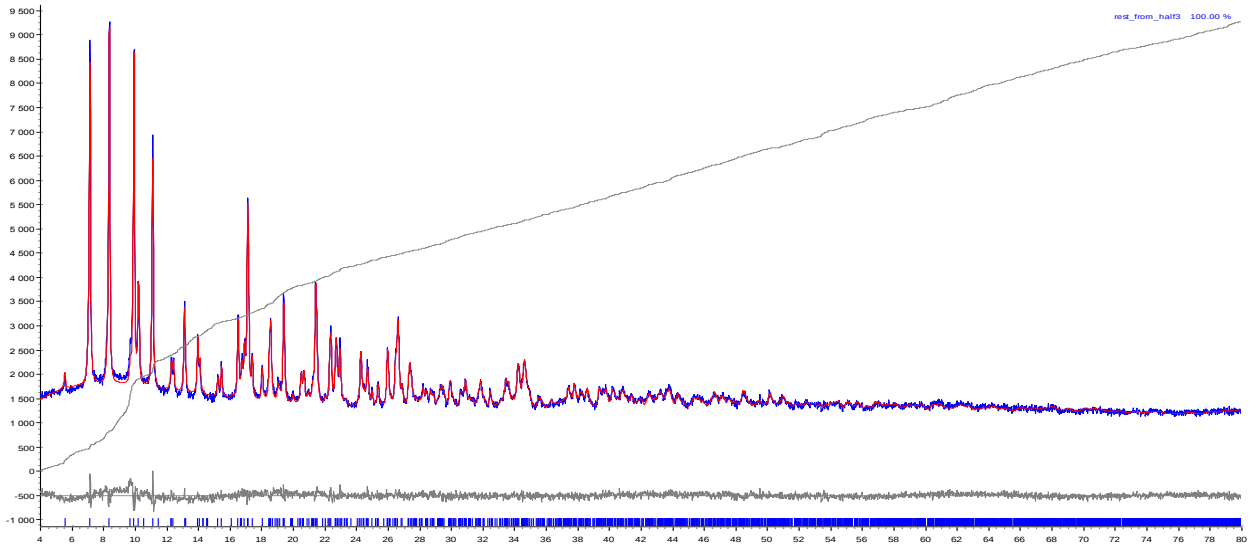

Figure 10 XRD patterns of Er(L)(HL)

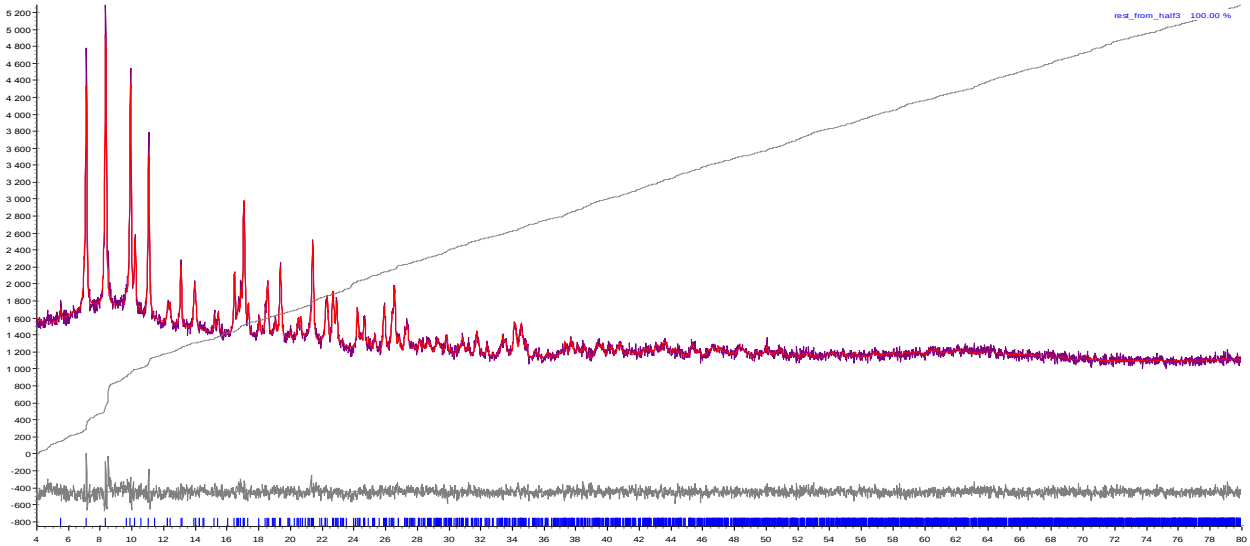

Figure 11 XRS patterns of Tb(L)(HL)

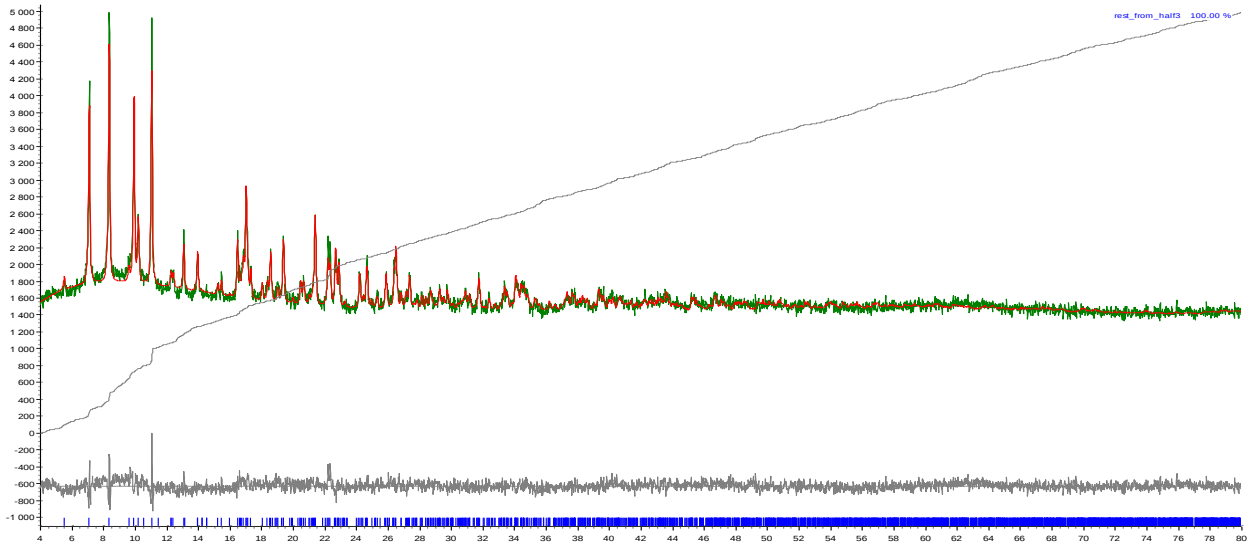

Figure 12 XRD patterns of Gd(L)(HL)

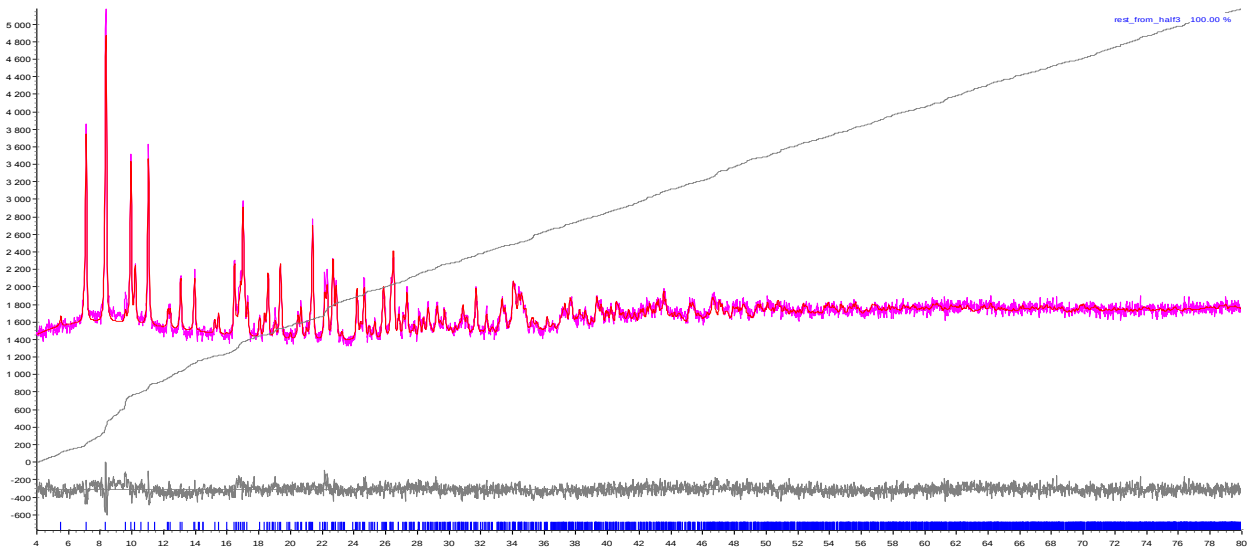

Figure 13 XRD patterns of Eu(L)(HL)

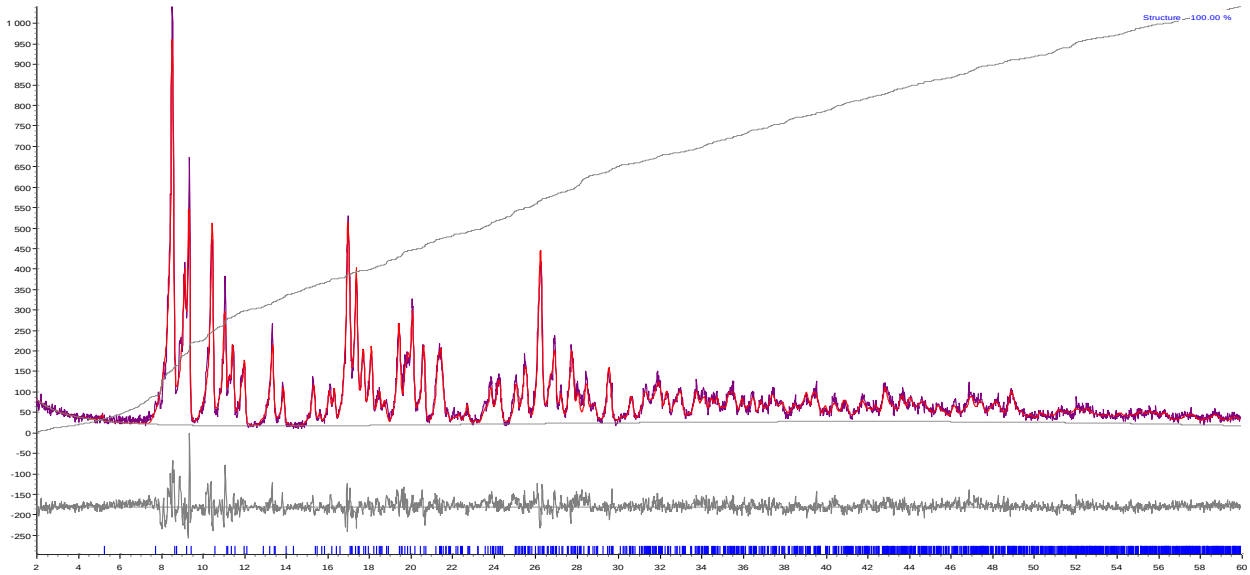

Figure 14 XRD patterns of Lu(HL)$_2$Cl

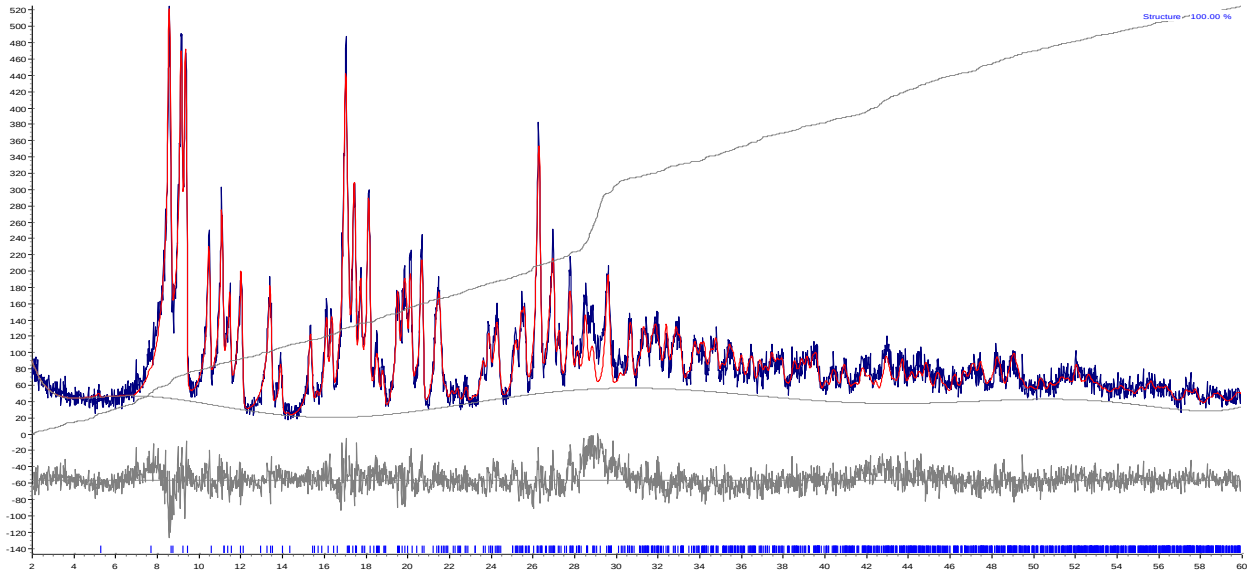

Figure 15 XRD patterns of $Yb(HL)_2Cl$

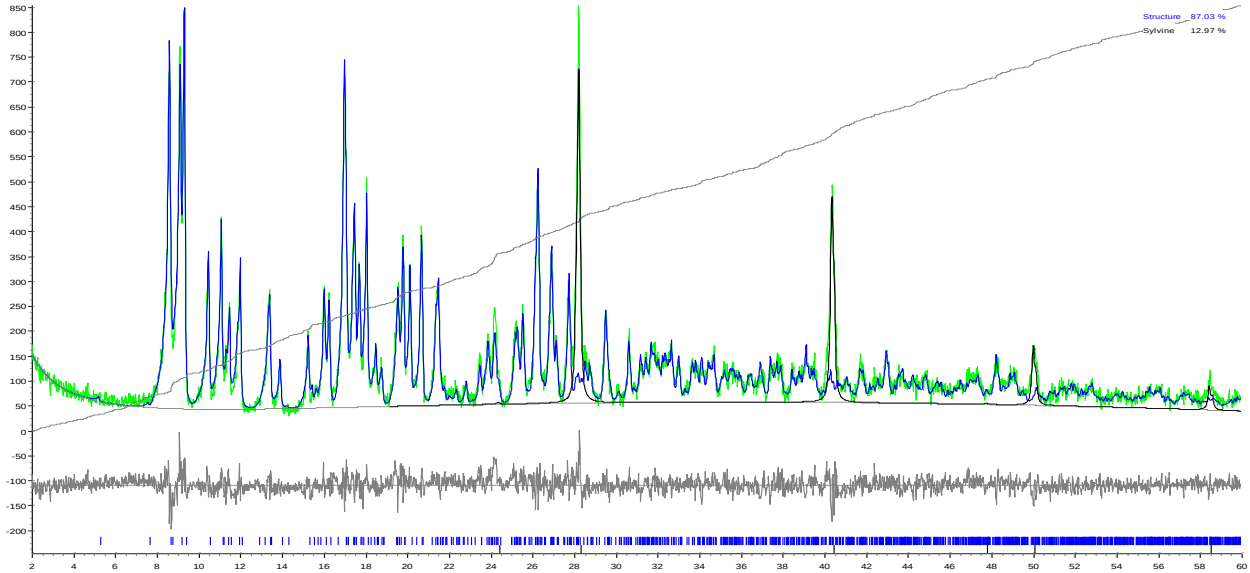

Figure 16 XRS patterns of $Er(HL)_2Cl$. Contains impurities of KCl.

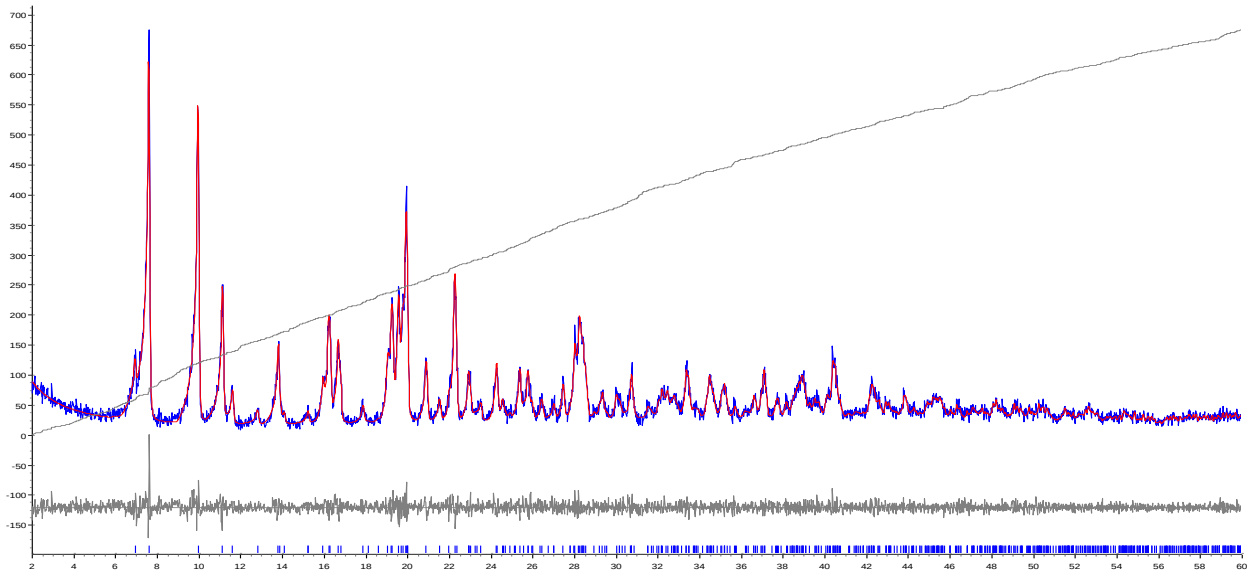

Figure 17 XRD patterns of $Tb(HL)_2Cl$

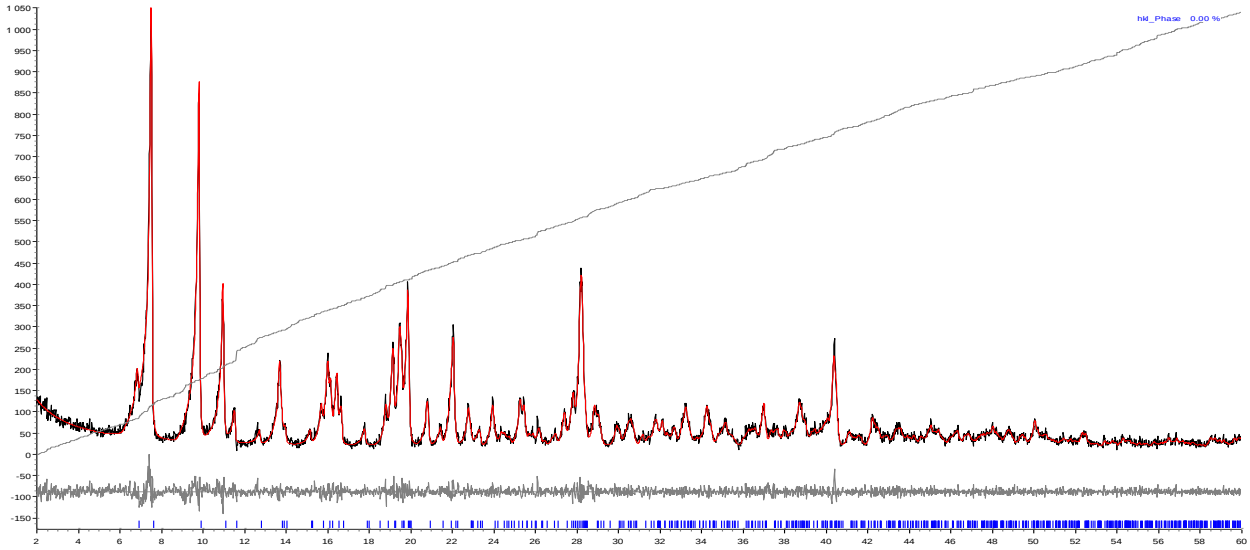

Figure 18 XRD patterns of $Eu(HL)_2Cl$

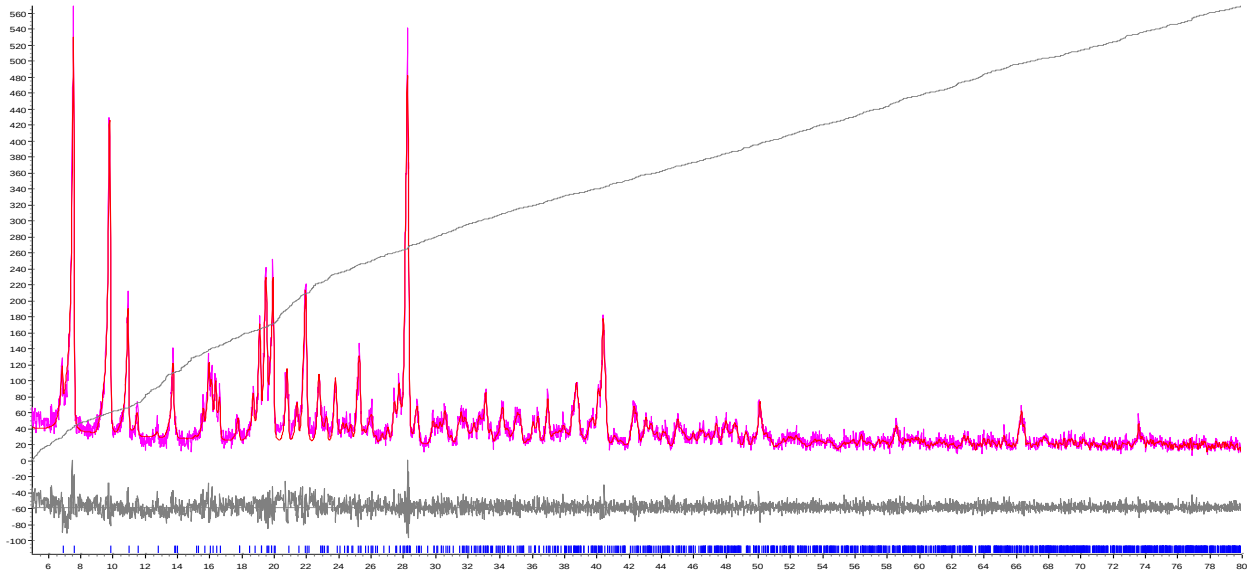

Figure 19 XRD patterns of $Nd(HL)_2Cl$

Integration of europium luminescence

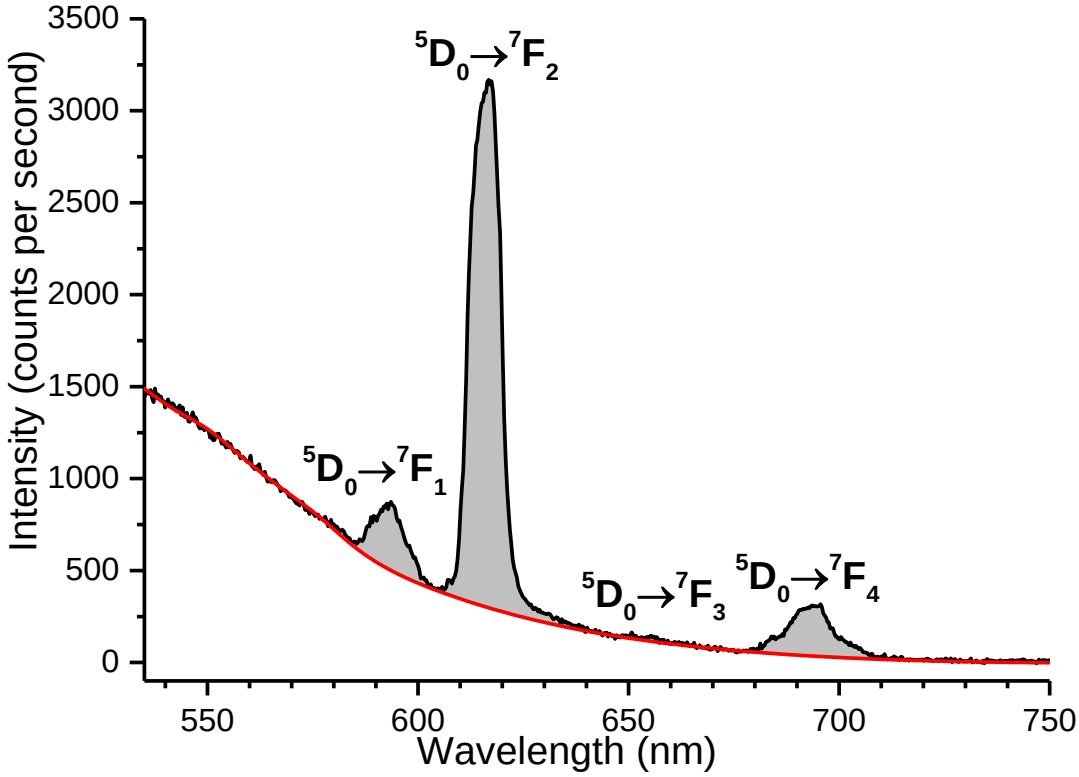

Figure 20 The integration of europium luminescence in the luminescence spectra of $Eu(HL)_2Cl$ at 167K. The bold curve is complex luminescence, the red curve is fitting of the organic luminescence.

The organic part of luminescence was fitted with B-spline function. The bands of $^5D_0 \rightarrow {}^7F_J$ (J = 1–4) transitions were integrated with the fitted organic luminescence as a baseline (see Figure 20 as an example) and summarized to give the integrated europium luminescence intensity. The same procedure was run for the spectra of Eu(L)(HL) in the range 77-200 K and $Eu(HL)_2Cl$ in the range 77-240 K, where europium luminesce could still be observed. The integration were made using Origin Pro 9.0 software.

IR spectroscopy

IR spectra in the ATR mode were recorded on a spectrometer SpectrumOne (Perkin-Elmer) in the region of 400-4000 cm^{-1}.

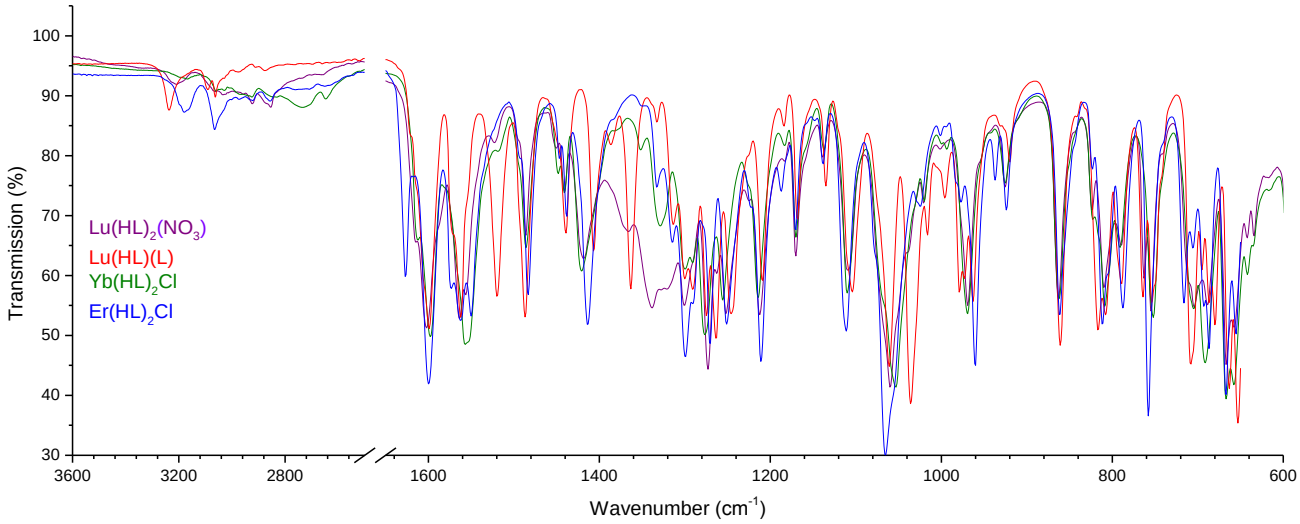

Figure 21 The IR spectra of the complexes

Luminescence spectra with time delay

Luminescence spectra with time delay were measured using Fluorolog 3 spectrofluorometer.

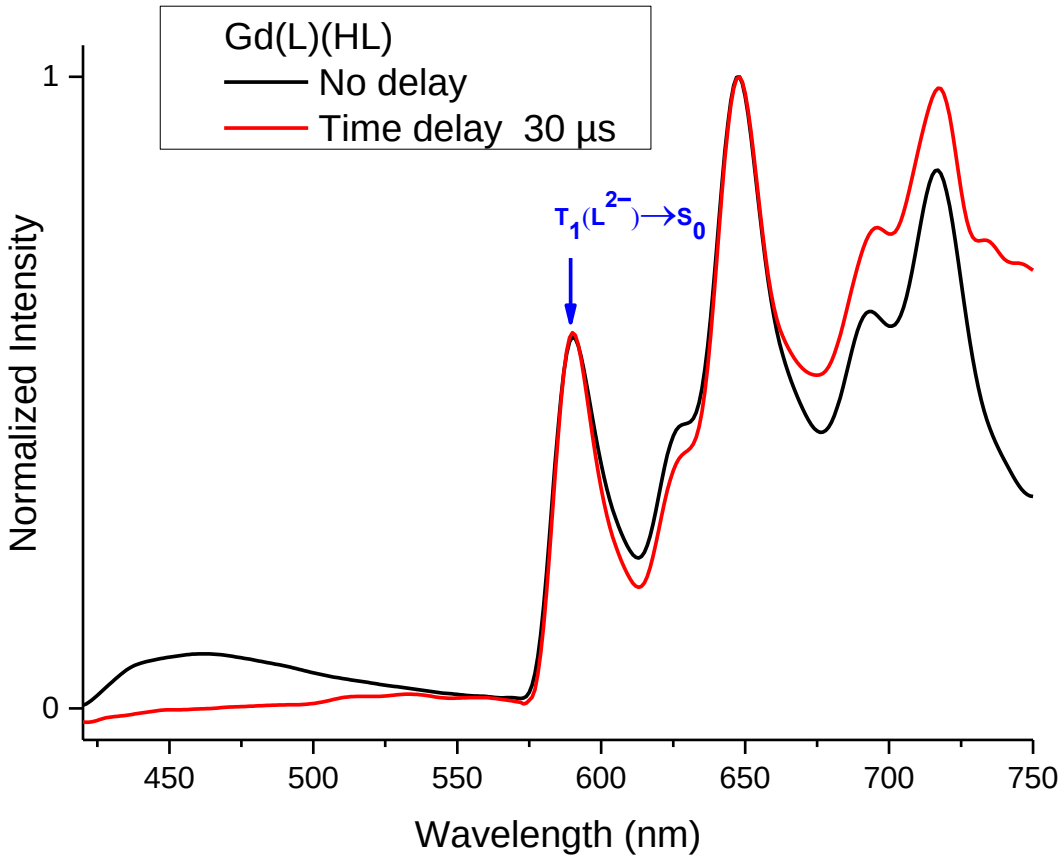

Figure 22 The luminescence spectra of Gd(L)(HL) in powder at 77K without time delay (black) and with 50 µs time delay (red)

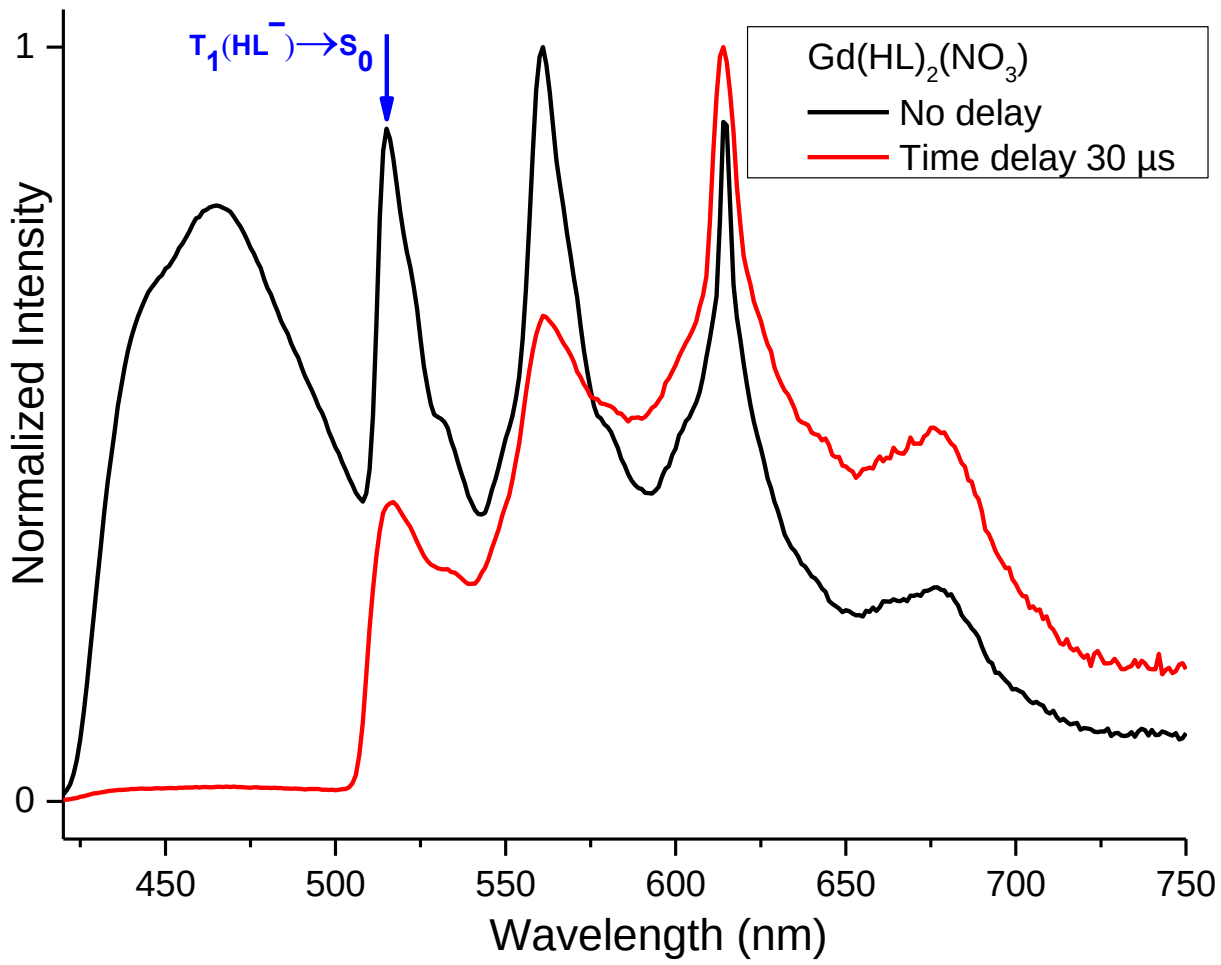

Figure 23 The luminescence spectra of $Gd(HL)_2(NO_3)$ in powder at 77K without time delay (black) and with 30 µs time delay (red)

The coordination environment of lanthanide ion

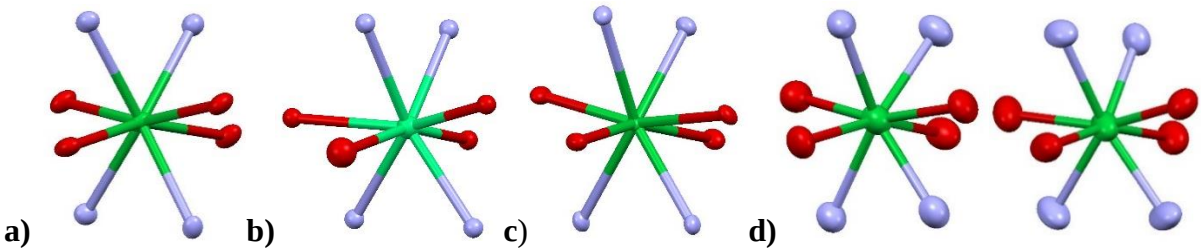

Figure 24 The coordination environment of metal ion in a) $Lu(HL)_2Cl$, b) Er(L)(HL), c) $Yb(L)(HL)(EtOH)_2(H_2O)$, d) $Yb(L)(HL)(H_2O)_2$. Oxygen atoms are red, nitrogen atoms are blue.

Literature

1. Sheldrick G.M. *SHELXT* – Integrated space-group and crystal-structure determination // Acta Crystallogr. Sect. A Found. Adv. 2015. Vol. 71, № 1. P. 3–8.

2. Sheldrick G.M. Crystal structure refinement with *SHELXL* // Acta Crystallogr. Sect. C Struct. Chem. 2015. Vol. 71, № 1. P. 3–8.

3. Sheldrick G. A short history of SHELX // Acta Crystallogr. Sect. A. 2008. Vol. 64, № 1. P. 112–122.

4. Coelho A.A. Indexing of powder diffraction patterns by iterative use of singular value decomposition // J. Appl. Crystallogr. 2003. Vol. 36, № 1. P. 86–95.

5. Bruker. TOPAS 5.0 User Manual. Karlsruhe, Germany: Bruker AXS GmbH, 2014.

6. Favre-Nicolin V., Černý R. FOX, `free objects for crystallography': a modular approach to ab initio structure determination from powder diffraction // J. Appl. Crystallogr. 2002. Vol. 35, № 6. P. 734–743.

7. Toraya H. Weighting Scheme for the Minimization Function in Rietveld Refinement // J. Appl. Crystallogr. 1998. Vol. 31, № 3. P. 333–343.

8. Dmitrienko A.O., Bushmarinov I.S. Reliable structural data from Rietveld refinements *via* restraint consistency // J. Appl. Crystallogr. 2015. Vol. 48, № 6. P. 1777–1784.